Peer-reviewed version available at *Int. J. Mol. Sci.* **2018**, *19*, 1261; doi:10.3390/ijms19041261

Article

Cytokine expression and macrophage localization in xenograft and allograft tumor models stimulated with lipopolysaccharide

Junko Masuda[1], Tsukasa Shigehiro[2], Takuma Matsumoto[3], Ayano Satoh[4], Akifumi Mizutani[5], Chiho Umemura[6], Shoki Saito[7], Mayumi Kijihira[8], Eiji Takayama[9], Akimasa Seno[10], Hiroshi Murakami[11], Masaharu Seno[12]

[1] Department of Medical Bioengineering, Graduate School of Natural Science and Technology, Okayama University, Okayama 700-0080, Japan. junkomasuda@okayama-u.ac.jp.
[2] Department of Medical Bioengineering, Graduate School of Natural Science and Technology, Okayama University, Okayama 700-0080, Japan. en20727@s.okayama-u.ac.jp.
[3] Department of Medical Bioengineering, Graduate School of Natural Science and Technology, Okayama University, Okayama 700-0080, Japan. pvxn4t5n@s.okayama-u.ac.jp.
[4] Department of Medical Bioengineering, Graduate School of Natural Science and Technology, Okayama University, Okayama 700-0080, Japan. ayano113@cc.okayama-u.ac.jp.
[5] Department of Medical Bioengineering, Graduate School of Natural Science and Technology, Okayama University, Okayama 700-0080, Japan. mizut-a@cc.okayama-u.ac.jp.
[6] Department of Medical Bioengineering, Graduate School of Natural Science and Technology, Okayama University, Okayama 700-0080, Japan. pmyu2alv@s.okayama-u.ac.jp.
[7] Department of Medical Bioengineering, Graduate School of Natural Science and Technology, Okayama University, Okayama 700-0080, Japan. p4hi0alp@s.okayama-u.ac.jp.
[8] Department of Applied Chemistry and Biotechnology, Faculty of Engineering, Okayama University, Okayama, Japan. pvc15we6@s.okayama-u.ac.jp.
[9] Department of Oral Biochemistry, Asahi University School of Dentistry, Gifu, Japan. takayama@dent.asahi-u.ac.jp.
[10] Department of Medical Bioengineering, Graduate School of Natural Science and Technology, Okayama University, Okayama 700-0080, Japan. aseno@okayama-u.ac.jp.
[11] Department of Medical Bioengineering, Graduate School of Natural Science and Technology, Okayama University, Okayama 700-0080, Japan. muraka-h@cc.okayama-u.ac.jp.
[12] Department of Medical Bioengineering, Graduate School of Natural Science and Technology, Okayama University, Okayama 700-0080, Japan. mseno@okayama-u.ac.jp.

* Correspondence: Junko Masuda, Department of Medical Bioengineering, Graduate School of Natural Science and Technology, Okayama University, Okayama 7008530, Japan; junkomasuda@okayama-u.ac.jp; Tel.: +81-86-251-8969, Fax: +81-86-251-8969

Received: 26 March 2018; Accepted: date; Published: date

Abstract: Macrophages and dendritic cells (DCs) acquire functionally distinct properties in response to various environmental stimuli; the interaction of these cells with myeloid-derived suppressor cells (MDSCs) in tumor microenvironments regulates cancer progression. Immunodeficient mice lacking T cells are less likely to reject human cancer cells because of major histocompatibility complex (MHC) mismatches. The xenograft tumor microenvironment, comprising human cancer and mouse host cells, exhibits more complex bidirectional signaling and function than a syngeneic tumor microenvironment. Here human and mouse colorectal cancer cells were transplanted into nude mice to elucidate differences in macrophage, DC, and MDSC functions in human xenograft and mouse allograft tumor models. Plasma interferon-γ and interleukin-18 concentrations in the former model after intraperitoneal lipopolysaccharide (LPS) administration were significantly higher than those in the latter model and non-transplanted control group. Splenic MHC class I, II, and CD80 expression increased in $CD11b^+$ and MDSC populations after LPS administration in only

Peer-reviewed version available at Int. J. Mol. Sci. 2018, 19, 1261; doi:10.3390/ijms19041261

the xenograft tumor model. The number of CD80- and MRC1-expressing cells decreased upon LPS administration in only the xenograft tumor. These results suggxest that macrophages and DCs function normally in xenograft tumor models, whereas their functions in response to LPS administration vary in allograft tumor models.

Keywords: Myeloid-derived suppressor cells (MDSCs); dendritic cells (DCs); M1 macrophages; M2 macrophages; xenograft tumor; allograft tumor; lipopolysaccharide (LPS)

1. Introduction

Many human cancer cell lines derived from patients have been established and studied over the past 40 years. In this cancer research, the transplantation of xenografts of patient-derived cancer cell lines into immunodeficient mice is commonly used to produce *in vivo* preclinical models for preclinical drug evaluation, biomarker identification, biologic studies, and personalized medicine strategies [1]. Because T cells are mainly mediate xenograft rejection, immunodeficient mice lacking T cells, known as nude mice, are frequently used for patient-derived cancer research; moreover, these mice express myeloid cells, such as macrophages myeloid-derived suppressor cells (MDSCs) and dendritic cells (DCs), which regulate cancer progression [2].

Macrophages can be divided into two major, distinct phenotypes based on their microenvironment. The M1 phenotype macrophages are pro-inflammatory and cytotoxic and are activated by gram-negative bacterial endotoxin lipopolysaccharide (LPS) or pro-inflammatory cytokines such as interferon (IFN)-γ and tumor necrosis factor-α (TNF-α) [3]. Thus, M1 macrophages have the potential to eliminate tumor cells. In contrast, M2 phenotype macrophages are activated by anti-inflammatory cytokines such as interleukin (IL)-4 and IL-13 and express high number of C-type mannose receptor 1 (MRC1). M2 macrophages are thought to be synonymous with tumor-associated macrophages (TAM) because they modulate inflammatory responses by decreasing responsiveness to toll-like receptors (TLRs) and IFN-γ [2,4–7].

MDSCs represent a heterogeneous cell population whose members share a capacity to exert a suppressor function [8–10] and whose numbers increase with the growth of human and murine cancers [11–16]. Although MDSCs are characterized by the dual expression of Gr-1 and CD11b in mice and are regarded as a distinct population from M2 macrophages, they share many characteristics in terms of mechanisms that sustain and promote tumor growth [2]. The experimental xenogeneic tumor microenvironment generated in immunodeficient mice consists of mouse stromal cells and these myeloid cells. However, the commonalities of the distributions and functions of M1 / M2 macrophages, DCs, and MDSCs between xenograft and allograft tumors are still controversial.

In this study, we established human xenograft and murine allograft tumor models in nude mice using human and murine colorectal adenocarcinoma cell lines and found that the xenograft tumor model can produce higher levels of pro-inflammatory cytokines when stimulated by LPS but not the allograft tumor model.

2. Results

2.1 *Expression of immune cells in nude mice*

We first characterized the population of immune cells in the spleens of nude mice, and both $CD4^+$ and $CD8^+$ T cells were absent (data not shown). As shown in Figure 1, major histocompatibility complex (MHC) class I and II molecules and the co-stimulatory molecule, CD80, are required for T cell activation and are highly expressed in M1 macrophages; these were observed in the $CD11b^+$ cell

Preprints (www.preprints.org) | NOT PEER-REVIEWED | Posted: 27 March 2018 doi:10.20944/preprints201803.0224.v1

Peer-reviewed version available at Int. J. Mol. Sci. 2018, 19, 1261; doi:10.3390/ijms19041261

population [17,18]. Splenic MHC class I expression on CD11b$^+$ cells increased following LPS stimulation in both wild type (WT) and nude mice (Figure 1A). These observations correlated with the MHC class II and CD80 expression on CD11b$^+$ cells (Figure 1B, C).

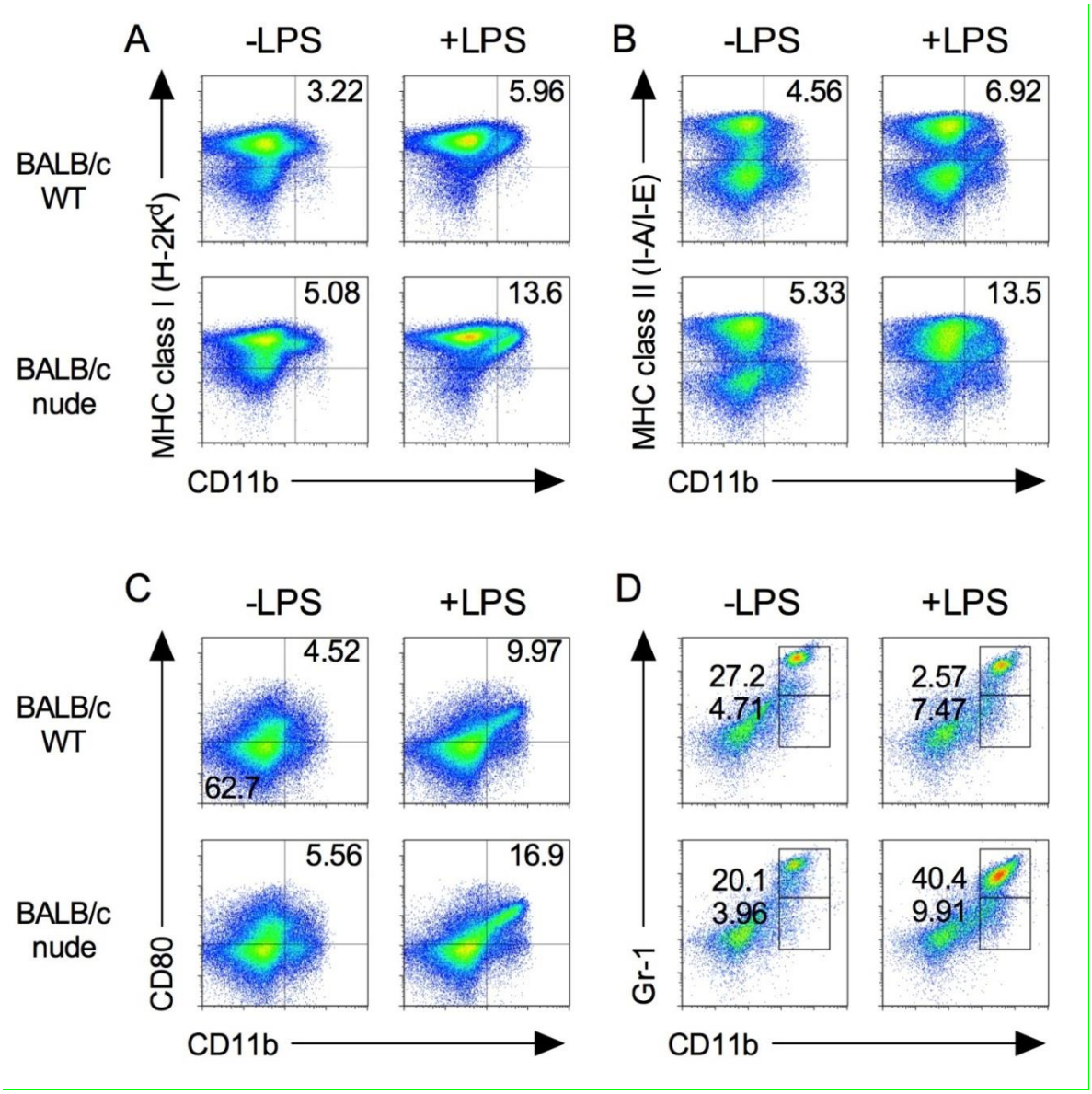

Figure 1. Expression of immune cells in BALB/c-nude mice. Splenocytes were isolated from spleen from BALB/c and BALB/c-nude mice after 24 h from i.p. injection of 500 μg LPS (+LPS) or PBS control (–LPS). The expression level of MHC class I (A), class II (B), CD80 (C), and Gr-1 (D) on CD11b$^+$ cells was analyzed by flow cytometry. Results shown are representative of at least three independent experiments.

In addition, MDSCs were identified by the co-expression of the myeloid lineage differentiation antigens Gr-1 and CD11b of mice [19,20]. The percentages of Gr-1^{dim} CD11b$^+$ and Gr-1^{hi} CD11b$^+$ MDSCs in nude mice were higher than those in WT mice (Figure 1D). These results suggest that M1 macrophages and MDSCs are functional in nude mice.

2.2 *Pro-inflammatory cytokine production in nude mice stimulated by LPS*

The pro-inflammatory cytokines TNF, IL-12, and IL-18 are mainly produced by macrophages and DCs, whereas IFN-γ is produced by natural killer (NK) cells. We determined the kinetics of the cytokine levels in peripheral blood after LPS injection. As shown in Figure 2A, the serum level of TNF was highest at 1 h and decreased to basal levels at 3 h, whereas that of IFN-γ was highest at 6 h and then gradually decreased (Figure 2B). In contrast, the serum level of IL-18 did not vary over the course of 24 h after LPS injection (Figure 2C). The serum levels of IL-1β and IL-12 were undetectable by ELISA (data not shown). Thus, we decided to use peripheral blood collected at 1 (for TNF), 3, 6, 9, 12, and 24 h (for IFN-γ and IL-18) after LPS injection for analysis in the subsequent experiment.

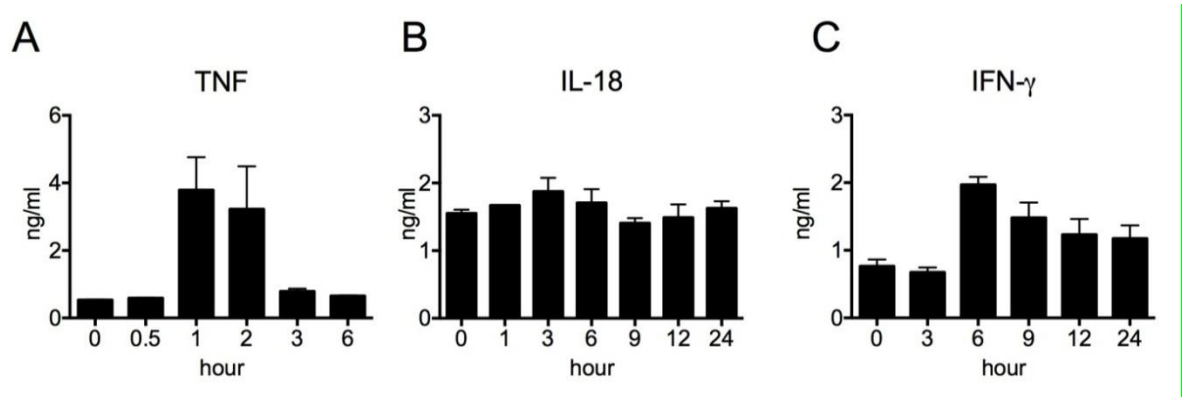

Figure 2. pro-inflammatory cytokine productions in nude mice stimulated by LPS. LPS was i.p. injected and blood samplings were carried out at indicated hour. The serum levels of TNF (A), IFN-γ (B) and IL-18 (C) were determined by ELISA. The data are presented as the mean ± SEM. n=5.

2.3 *Serum pro-inflammatory cytokine levels in the xenograft tumor model after LPS stimulation*

To examine the respective cytokine production in the xenograft tumor model, we subcutaneously injected human colon adenocarcinoma cell lines (HT29) or PBS (as a control) into nude mice and then intraperitoneally injected LPS at 21 d after inoculation. As shown in Figure 3A and C, the serum levels of TNF and IFN-γ significantly increased in HT29 tumor-bearing mice at 1 h (TNF) and at 3 to 6 h (IFN-γ). Furthermore, the serum level of IL-18 also significantly increased in HT29 tumor bearing mice at 6 to 12 h (Figure 3B). These results suggested that HT29 tumor-bearing mice have more potential to promote pro-inflammatory responses than sham control mice.

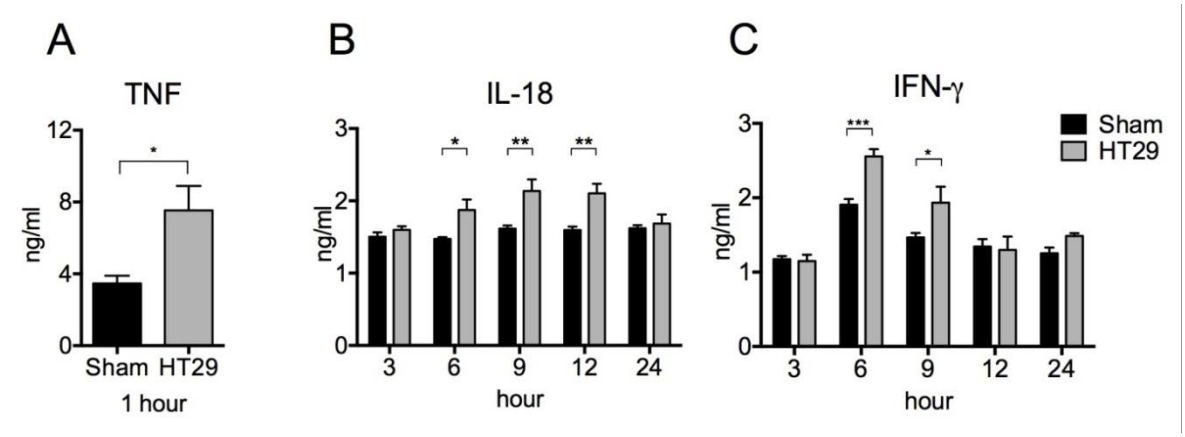

Peer-reviewed version available at Int. J. Mol. Sci. 2018, 19, 1261; doi:10.3390/ijms19041261

Figure 3. Increased serum pro-inflammatory cytokine levels in xenograft tumor mice after LPS stimulation. HT29 cells or PBS were injected subcutaneously (s.c.) into BALB/c-nu/nu mouse. On the day 21 after tumor transplantation, 500 μg LPS was i.p. injected into the xenograft mice and peripheral blood was collected at indicated hour. The serum levels of TNF (A), IFN-γ (B), and IL-18 (C) were detected by ELISA. The data are presented as the mean ± SEM assessed by a Student's two-tailed *t*-test. *p<0.05; **p<0.01; ***p<0.001. n=5.

2.4 *Serum pro-inflammatory cytokine levels in the allograft tumor model were unchanged even after LPS stimulation*

Given the increased production of pro-inflammatory cytokines in HT29 tumor-bearing nude mice, we next studied the respective cytokine production in the xenograft and allograft tumor models after LPS treatment. To this end, we subcutaneously injected human or mouse colon adenocarcinoma cell lines (HT29 or CT26) in nude mice. Interestingly, as shown in Figure 4B and C, the serum levels of IL-18 and IFN-γ of CT26 tumor-bearing mice did not increase whereas the serum level of TNF was as high as HT29 tumor-bearing mice (Figure 4A). Thus, the potential for pro-inflammatory responses in the xenograft tumor model is much greater than in the allograft model.

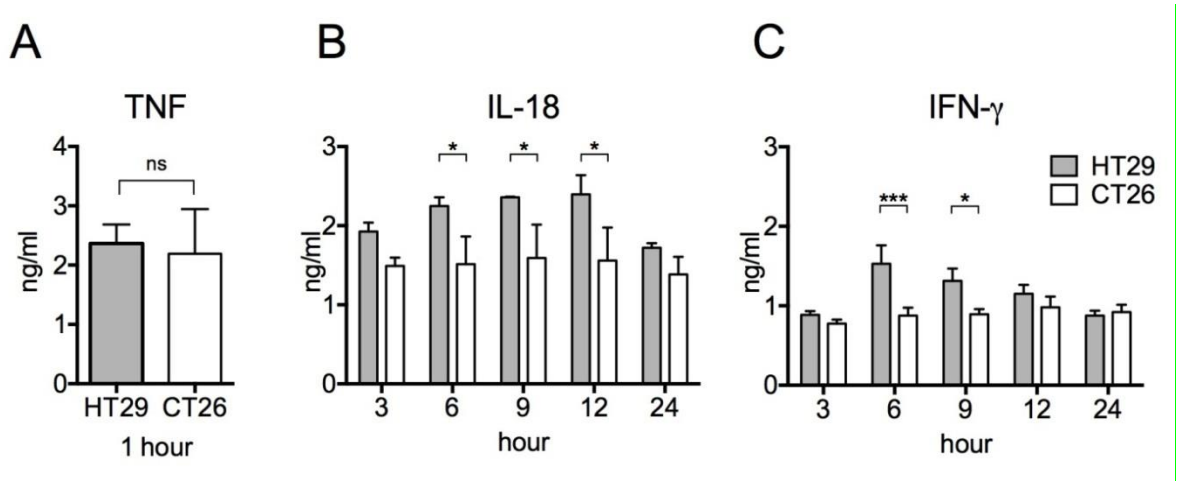

Figure 4. Unchanged serum pro-inflammatory cytokine levels in allograft tumor models even after LPS stimulation. HT29 cells or CT26 cells were transplanted subcutaneously (s.c.) into BALB/c-nu/nu mice. On the day 21 after transplantation, 500 μg LPS was i.p. injected and peripheral blood was collected at indicated hour. The serum levels of TNF (A), IFN-γ (B), and IL-18 (C) were detected by ELISA. The data are presented as the mean ± SEM assessed by a Student's two-tailed *t*-test. *p<0.05; ***p<0.001; ns: not significant. n=5.

2.5 *Splenic M1 macrophages and MDSCs increase after LPS stimulation in the xenograft tumor model*

The spleen traps pathogens and antigens in circulating blood and initiates innate and adaptive immune responses. Macrophages exist in the spleen in a steady state, whereas MDSCs migrate there during inflammation or cancer progression [16,18]. To determine the differences in the expression and functions of M1 macrophages and MDSC subsets, HT29 and CT26 tumor-bearing mice were administered with LPS as described above, and their splenocytes were stained for M1 macrophages. As shown in Figure 5A-C, MHC class I, II, and CD80 expression on $CD11b^+$ cells

Preprints (www.preprints.org) | NOT PEER-REVIEWED | Posted: 27 March 2018 doi:10.20944/preprints201803.0224.v1

Peer-reviewed version available at Int. J. Mol. Sci. 2018, 19, 1261; doi:10.3390/ijms19041261

increased in HT29 tumor-bearing mice following LPS injection, whereas MHC class I and II expression on CD11b$^+$ cells remained unchanged in CT26 tumor-bearing mice following LPS injection. Notably, LPS injection decreased CD80 expression on CD11b$^+$ cells in CT26 tumor-bearing mice (Figure 5A-C).

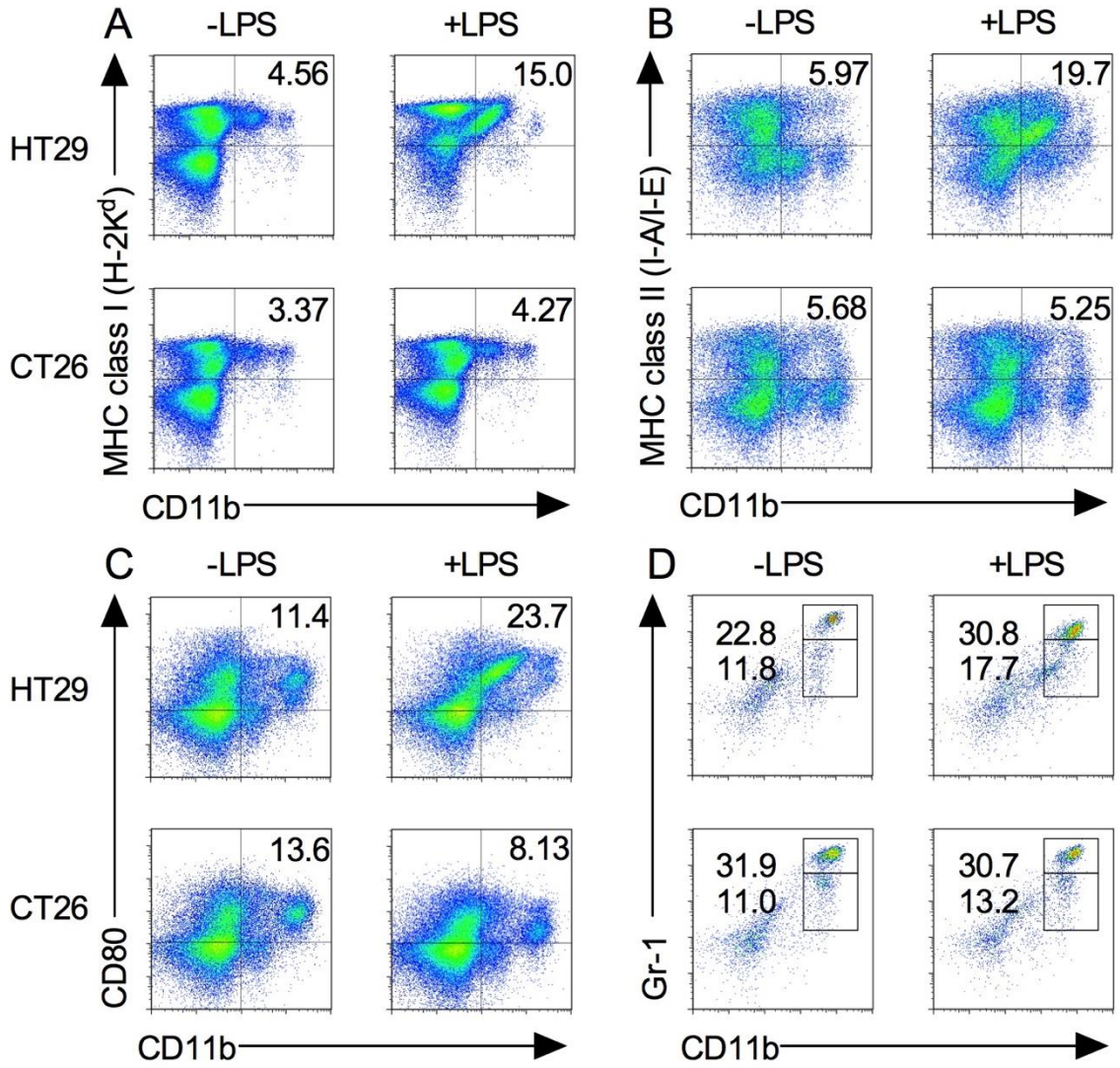

Figure 5. M1 macrophages and MDSCs in xenograft and allograft tumor models after LPS stimulation. HT29 and CT26 tumor-bearing mice were treated with LPS on the day 21 from tumor transplantation and splenocytes were isolated at 24 h. The expression level of MHC class I (A), class II (B), CD80 (C), and Gr-1 (D) on CD11b$^+$ cells was analyzed by flow cytometry. Results shown are representative of at least three independent experiments.

We next examined the splenic MDSC population. Compared with the steady state (Figure 1D), the percentage of MDSCs in HT29 tumor-bearing mice slightly increased during tumor growth and even further after LPS injection (Figure 5D). In contrast, the percentage of MDSCs in CT26 tumor-bearing mice increased dramatically during tumor growth, and there was no observed difference following LPS injection (Figure 5D). Taken together, these results indicated that the

functions of these splenic myeloid cells were different between xenograft and allograft tumor models.

2.6 *Expression of tumor-infiltrated M1 and M2 macrophages before and after induction by LPS*

M1 macrophages and activated DCs express CD80, whereas M2 macrophages express MRC1. Additionally, CD80 is also expressed on activated DCs. To investigate the localization and function of M1/M2 macrophages in the spleens and tumors of HT29 and CT26 tumor-bearing mice, we stained spleen and tumor sections with M1 and M2 macrophage markers, CD80 and MRC1, respectively. In the spleens of HT29 tumor-bearing mice, CD80 expressing cells were very few and MRC1-expressing cells were dominant at steady state (Figure 6A). Following exposure to LPS, the number of CD80-expressing cells increased and that of MRC1 expressing cells decreased (Figure 6A). In tumors of HT29 tumor-bearing mice, CD80-expressing-cells predominantly localized with tumor cells, and MRC1-expressing cells were also present at steady state (Figure 6B). Following exposure to LPS, the number of CD80- and MRC1-expressing cells decreased (Figure 6B). In the spleens of CT26 tumor-bearing mice, CD80- and MRC1-expressing cells were present; they did not increase following exposure to LPS (Figure 6C). Notably, very few CD80-expressing cells and many MRC1-expressing cells were present in the CT26 tumor compared with the HT29 tumor, and their levels did not change following LPS exposure (Figure 6D). Taken together, these results suggest that the physiological function of CD80-expressing cells after LPS signaling was retained in the xenograft tumor model but not the allograft tumor model.

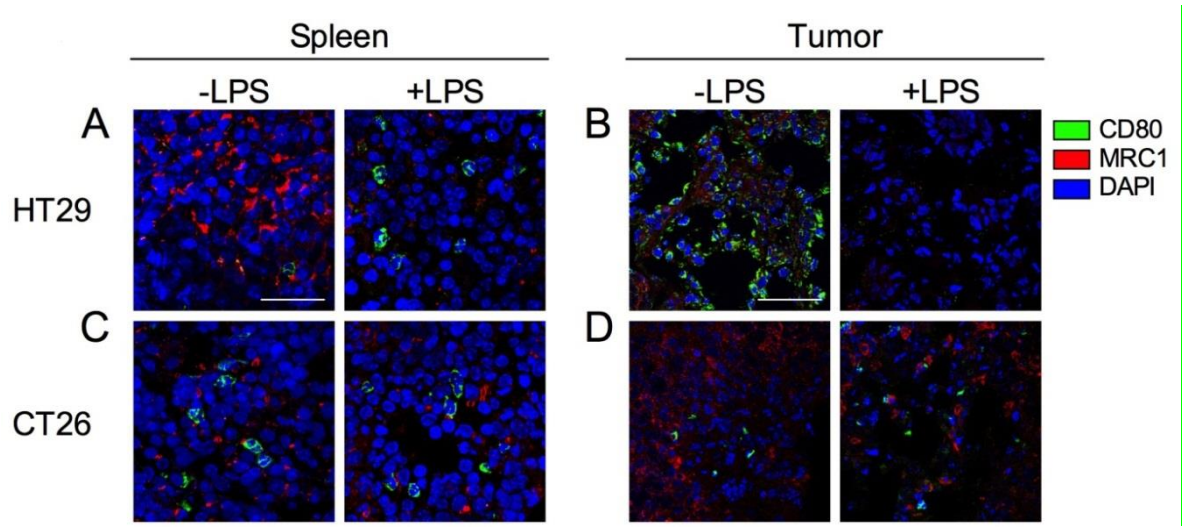

Figure 6. Confocal images of CD80 and MRC1 expression cells in spleen and tumor with or without injection of LPS. HT29 and CT26 tumor-bearing mice were treated with LPS (+LPS) or PBS control (–LPS) on the day 21 from tumor transplantation and tumor and spleen were collected after 24 h from LPS treatment. (A) Spleen in HT29 tumor-bearing mice. (B) Tumor in HT29 tumor-bearing mice. (C) Spleen in CT26 tumor-bearing mice. (D) Tumor in CT26 tumor-bearing mice. CD80, MRC1, and cell nuclei (DAPI) are represented in green, red, and blue, respectively. Results shown are representative of at least three independent experiments. Each scale bar shows 50 μm.

3. Discussion

Macrophages and MDSCs play an important role in systemic and tumor immunity. Thus, using patient-derived tumor cell lines in xenograft experiments has contributed to our understanding of

the mechanisms of macrophage infiltration into tumors [21]. However, the xenograft tumor microenvironment is composed of human and murine cells, and this species mismatch might result in more complicated bidirectional signaling and function in the stromal cells compared with syngeneic tumor microenvironments. In this study, we tried to clarify the difference with respect to M1/M2 macrophages, DCs, and MDSCs between xenograft and allograft tumor models and found that the xenograft tumor model produces more pro-inflammatory cytokines than the allograft tumor model.

After being primed by LPS, macrophages and DCs become activated through TLR4-mediated cytokine production (TNF, IL-12, and IL-18) and surface expression of several stimulating ligands such as MHC molecules and CD80, leading to NK cell activation, which leads IFN-γ production [22]. More recently, it has been realized that LPS directly stimulates IFN-γ production in NK cells independently of the established TLR4-mediated signaling pathway [23]. The LPS injections we utilized in this study were an appropriate way to probe macrophage and DC function in the tumor models because LPS drives macrophages to a preferentially M1 phenotype [24,25].

LPS administered i.p. is rapidly absorbed into the systemic circulation [26] and reaches other organs, including tumors, and is trapped in the spleen, which hosts macrophages and DCs [18,27]. Similarly, when tumor antigens produced during tumor cell apoptosis reach systemic circulation, they are eventually filtered through the spleen. Interestingly, we found that there was a significant increase of the IL-18 and IFN-γ in the sera of xenograft tumor model mice after LPS stimulation compared with sham mice (Figure 4) and allograft model mice (Figure 5). Our study also showed that the pro-inflammatory states in the spleen and tumor in the xenograft and allograft tumor models were completely different even before LPS administration (Figure 7). These results indicate that the function of M1 macrophages and production of pro-inflammatory cytokines against tumors in the xenograft tumor models are elevated even when T cells are absent and that tumor phagocytosis by macrophages was adequately induced in the tumor environment of the xenograft tumor model, whereas macrophage-mediated tumor destruction was inhibited and splenic chronic inflammation was induced the allograft tumor model [28–30]. One of the reasons is that MDSCs were not induced by cancer growth in the xenograft model, whereas they were induced by LPS (Figure 5). MDSCs, TAMs, and some DC populations suppress immune activity, which is enhanced by their interactions with each other [25]. Although accumulation of MDSCs occurs via chronic inflammation, it is quite interesting that MDSCs did not increase during xenograft tumor growth. Human tumor cells do not express mouse MHC class I molecules that are recognized by mouse immune cells such as NK cells [31]. Although NK cells can be converted into MDSCs in allograft tumor models, this conversion is inhibited by the presence of IL-2 [32]. These reports suggest that an unknown mechanism of cell-to-cell contact involving MHC-dependent signaling is required to regulate MDSCs in systemic and tumor microenvironments and that these mechanisms might induce different immune responses in xenograft and allograft tumor models [25,33].

Our study showed that MRC1 expression in the spleen and tumor was repressed after LPS injection in the xenogeneic tumor model but did not change in allograft tumor (Figure 7). As IFN-γ suppresses the basal expression of genes that are homeostasis and reparative phenotypes of M2 macrophages, MRC1 expression in M2 macrophages could be suppressed following their expression [34]. In addition to the plasticity of M1 macrophages in phenotype conversion into M2 macrophages, fully polarized M2 macrophages can be converted into M1 macrophages that produce inflammatory cytokines following stimulation by LPS [35]. Our results indicated that not only M1 macrophages but also M2 macrophages function properly in the xenograft tumor model, whereas the function of both macrophages is lost in the allograft tumor model. The influence of M2 macrophages of allograft tumor models lacking the ability to convert into M1 macrophages in systemic and tumor microenvironments needs to be extensively studied in the future.

Cancer research using xenograft tumor models is important for the elucidation of signal transduction in cancer cells and for screening candidate anti-cancer compounds. However, these results are not necessarily consistent with clinical outcomes [1]. Our results imply that one of the reasons for this might be that host immune responses generated in systemic and tumor microenvironments in xenograft models are quite different than in spontaneous tumor or allograft tumor implantation. In addition to the research focusing on the tumor microenvironment created by the presence of mouse stromal cells, research on signal transduction and drug screening might also be necessary to fully understand the influence of cell-to-cell contact of cells from different species.

4. Materials and Methods

4.1 *Reagents and antibodies (Abs)*

LPS (Lot. No. L8274) was purchased from Sigma-Aldrich (St. Louis, MO). Anti-mouse CD4 (RM4-5), CD11b (M1/70) and MHC Class I ($H2K^d$, SF1-1.1) monoclonal (m) Abs were purchased from BD Biosciences (San Jose, CA). Anti-mouse CD16/CD32 (93), and Gr-1 (RB6-8C5) mAbs were purchased from eBioscience (San Diego, CA). Anti-CD8α (53-6.7), CD11c (N418), CD80 (16-10A1), MHC Class II (I-A/I-E, M5/114.15.2) and 7-amino-actinomycin D (7AAD) from Tonbo Biosciences. Anti-MRC1 polyclonal (p) Ab was from Bioss Antibodies (Woburn, MA, USA).

4.2 *Animals*

Female BALB/c and BALB/c nu/nu mice were obtained from Charles River Inc. (Kanagawa, Japan) and maintained under specific pathogen-free conditions at the Tsushima-kita Branch, Department of Animal Resources, Advanced Research Center, Okayama University. All animal experiments were reviewed and approved by the ethics committee (Animal Care and Use Committee) for animal experiments of Okayama University under the project identification code IDs OKU-2015229 (12 May 2015), OKU-2016225 (6 June 2016) and OKU-2016361 (21 September 2016).

4.3 *LPS injection*

A total of 500 μg (for BALB/c) or a serial concentration (for BALB/c nu/nu) of LPS (in 200 μL PBS /body) was intraperitoneally (i.p.) injected and peripheral blood and tissue samplings were obtained within 24 h.

4.4 *Tumor cell cultures*

Colon adenocarcinoma cell lines, HT29 and CT26 were purchased from the American Type Culture Collection (Rockville, MD) and maintained in Roswell Park Memorial Institute (RPMI) 1640 medium (Sigma-Aldrich, St. Louis, MO) supplemented with 10 % (v/v) heat-inactivated fetal bovine serum (FBS) (SAFC Biosciences, Lenexa, KS) and 1 % (v/v) antibiotic-antimycotic solution (10,000 U/mL penicillin, 10,000 μg/mL streptomycin, and 25 μg/mL amphotericin B; Life Technologies, Gaithersburg, MD).

4.5 *Tumor cell implantations*

HT29 cells (3×10^6 cells/body) or CT26 cells (1×10^5 cells/body) in 200 μL PBS were implanted subcutaneously into the right flank of a 5-week-old female mouse. A sham mouse, as control experiments, was injected PBS alone. On the day 21, 500 μg LPS in 200 μL PBS was i.p. injected and peripheral blood and tissue samplings were obtained within 24 h.

4.6 *Assays for cytokine levels*

Mouse peripheral blood was centrifuged at 500 × g for 5 min. After clear plasma was collected, TNF, IFN-γ, and IL-18 levels were evaluated by using cytokine-specific enzyme-linked immunosorbent assay (ELISA) commercially available from BD Biosciences and BMN (Nagoya, Japan).

4.7 *Flow cytometry*

Splenocytes were isolated as according to a previously study [36]. Splenocytes (2×10^6) were incubated with anti-CD16/CD32 mAb for 20 min on ice then stained with anti-CD4 and CD8α, $H2K^d$, I-A/I-E, Gr-1 and CD11b for 30 min on ice followed by labelling with 7AAD. The stained cells were analyzed by Accuri™ (BD Biosciences) and FlowJo Software (Treestar, Inc., San Carlos, CA).

4.8 *Immunohistochemical analyses*

Tissues were placed in OTC compound (Miles Laboratories, Naperville, IL) and quickly frozen in liquid nitrogen and stored at -80°C. Frozen sections (6 μm) were fixed with 4% formaldehyde neutral buffer solution (Nacalai Tesque, Kyoto, Japan) for 15 min followed by permeabilisation with 0.1% Triton X-100 in PBS for 5 min and blocked with 4% BSA in PBS for 15 min at room temperature. The sections were then incubated with biotinylated anti-CD11b and FITC-labelled anti-MHC-Class II or anti-MRC Abs for 1 h. After washing in PBS, the sections were incubated with secondary antibodies for 15 min. The immunofluorescence images visualized under a confocal microscope (FV-1000, Olympus, Japan).

4.9 *Statistical analyses*

Statistical analyses were performed using the Student's two-tailed *t*. All analyses were performed using GraphPad Prism Software Version 6 (GraphPad Software Inc, San Diego, CA). P-values < 0.05 were considered to be statically significant.

Acknowledgments: This study was supported by Program to Disseminate Tenure Tracking System, MEXT, Japan, Ryobi Teien Foundation, Okayama Foundation for Science and Technology, Sanyo Hohso Foundation, TOBE MAKI Scholarship Foundation and the Wesco Scientific Promotion Foundation.

Author Contributions: Junko Masuda directed the whole study. Junko Masuda, Tsukasa Shigehiro, Ayano Satoh and Eiji Takayama designed the experiments. Junko Masuda, Takuma Matsumoto, Ayano Satoh, Shoki Saito, Chiho Umemura and Mayumi Kijihira performed the experiments. Junko Masuda, Ayano Satoh and Takuma Matsumoto analyzed the data. Eiji Takayama, Akifumi Mizutani and Hiroshi Murakami contributed supplying reagents and materials and supported analysis. Junko Masuda, Tsukasa Shigehiro, Eiji Takayama, Ayano Satoh, Akimasa Seno, Akifumi Mizutani, Hiroshi Murakami and Masaharu Seno participated in the discussion. Junko Masuda and Tsukasa Shigehiro wrote the manuscript.

Conflicts of Interest: The authors declare no financial or commercial conflict of interest.

Abbreviations

DAPI	4',6-diamidino-2-phenylindole
DCs	Dendritic cells
ELISA	Enzyme-linked immunosorbent assay
FBS	Fetal bovine serum
IFN	Interferon
I.p.	Intraperitoneally
LPS	Lipopolysaccharide
MDSCs	Myeloid-derived suppressor cells
MHC	Major histocompatibility complex
MRC1	C-type mannose receptor 1
NK	Natural killer
RPMI	Roswell park memorial institute
S.c.	Subcutaneously
TAM	Tumor-associated macrophages
TLRs	Toll-like receptors
TNF-α	Tumor necrosis factor-α
WT	Wild type

References

1. Hidalgo, M.; Amant, F.; Biankin, A. V; Budinská, E.; Byrne, A. T.; Caldas, C.; Clarke, R. B.; de Jong, S.; Jonkers, J.; Mælandsmo, G. M.; Roman-Roman, S.; Seoane, J.; Trusolino, L.; Villanueva, A. Patient-derived xenograft models: an emerging platform for translational cancer research. Cancer Discov. 2014, 4, 998–1013, doi:10.1158/2159-8290.CD-14-0001.
2. Ugel, S.; Sanctis, F. De; Mandruzzato, S.; Bronte, V. Tumor-induced myeloid deviation: when myeloid-derived suppressor cells meet tumor-associated macrophages. J. Clin. Invest. 2015, 125, 3365–3376, doi:10.1172/JCI80006.
3. Lu, G.; Zhang, R.; Geng, S.; Peng, L.; Jayaraman, P.; Chen, C.; Xu, F.; Yang, J.; Li, Q.; Zheng, H.; Shen, K.; Wang, J.; Liu, X.; Wang, W.; Zheng, Z.; Qi, C.-F.; Si, C.; He, J. C.; Liu, K.; Lira, S. A.; Sikora, A. G.; Li, L.; Xiong, H. Myeloid cell-derived inducible nitric oxide synthase suppresses M1 macrophage polarization. Nat. Commun. 2015, 6, 6676, doi:10.1038/ncomms7676.
4. Chen, W.; Wang, J.; Jia, L.; Liu, J.; Tian, Y. Attenuation of the programmed cell death-1 pathway increases the M1 polarization of macrophages induced by zymosan. Cell Death Dis. 2016, 7, e2115, doi:10.1038/cddis.2016.33.
5. Gordon, S. R.; Maute, R. L.; Dulken, B. W.; Hutter, G.; George, B. M.; McCracken, M. N.; Gupta, R.; Tsai, J. M.; Sinha, R.; Corey, D.; Ring, A. M.; Connolly, A. J.; Weissman, I. L. PD-1 expression by tumour-associated macrophages inhibits phagocytosis and tumour immunity. Nature 2017, 545, doi:10.1038/nature22396.
6. Zhang, B.; Yao, G.; Zhang, Y.; Gao, J.; Yang, B.; Rao, Z.; Gao, J. M2-polarized tumor-associated macrophages are associated with poor prognoses resulting from accelerated lymphangiogenesis in lung adenocarcinoma. Clinics (Sao Paulo). 2011, 66, 1879–86, doi:10.1590/S1807-59322011001100006.
7. Mantovani, A.; Sozzani, S.; Locati, M.; Allavena, P.; Sica, A. Macrophage polarization: tumor-associated macrophages as a paradigm for polarized M2 mononuclear phagocytes. Trends Immunol. 2002, 23, 549–555, doi:10.1016/S1471-4906(02)02302-5.
8. Youn, J.-I.; Nagaraj, S.; Collazo, M.; Gabrilovich, D. I. Subsets of Myeloid-Derived Suppressor Cells in Tumor-Bearing Mice. J. Immunol. 2008, 181, 5791–5802, doi:10.4049/jimmunol.181.8.5791.
9. Rutkowski, M. R.; Stephen, T. L.; Svoronos, N.; Allegrezza, M. J.; Tesone, A. J.; Perales-Puchalt, A.; Brencicova, E.; Escovar-Fadul, X.; Nguyen, J. M.; Cadungog, M. G.; Zhang, R.; Salatino, M.; Tchou, J.; Rabinovich, G. A.; Conejo-Garcia, J. R. Microbially driven TLR5-dependent signaling governs distal malignant progression through tumor-promoting inflammation. Cancer Cell 2015, 27, 27–40, doi:10.1016/j.ccell.2014.11.009.

10. Fichtner-Feigl, S.; Terabe, M.; Kitani, A.; Young, C. a; Fuss, I.; Geissler, E. K.; Schlitt, H.-J.; Berzofsky, J. a; Strober, W. Restoration of tumor immunosurveillance via targeting of interleukin-13 receptor-alpha 2. Cancer Res. 2008, 68, 3467–75, doi:10.1158/0008-5472.CAN-07-5301.
11. Wang, J. C.; Kundra, A.; Andrei, M.; Baptiste, S.; Chen, C.; Wong, C.; Sindhu, H. Myeloid-derived suppressor cells in patients with myeloproliferative neoplasm. Leuk. Res. 2016, 43, 39–43, doi:10.1016/j.leukres.2016.02.004.
12. Stiff, A.; Trikha, P.; Wesolowski, R.; Kendra, K.; Hsu, V.; Uppati, S.; McMichael, E. L.; Duggan, M.; Campbell, A.; Keller, K.; Landi, I.; Zhong, Y.; Dubovsky, J.; Howard, J. H.; Yu, L.; Harrington, B.; Old, M.; Reiff, S.; Mace, T.; Tridandapani, S.; Muthusamy, N.; Caligiuri, M.; Byrd, J. C.; Carson, W. E. Myeloid-derived suppressor cells express Bruton's tyrosine kinase and can be depleted in tumor bearing hosts by ibrutinib treatment. Cancer Res. 2016, doi:10.1158/0008-5472.CAN-15-1490.
13. Highfill, S. L.; Rodriguez, P. C.; Zhou, Q.; Goetz, C. a; Koehn, B. H.; Veenstra, R.; Taylor, P. a; Panoskaltsis-Mortari, A.; Serody, J. S.; Munn, D. H.; Tolar, J.; Ochoa, A. C.; Blazar, B. R. Bone marrow myeloid-derived suppressor cells (MDSCs) inhibit graft-versus-host disease (GVHD) via an arginase-1-dependent mechanism that is up-regulated by interleukin-13. Blood 2010, 116, 5738–47, doi:10.1182/blood-2010-06-287839.
14. Chen, S.; Akbar, S. M. F.; Abe, M.; Hiasa, Y.; Onji, M. Immunosuppressive functions of hepatic myeloid-derived suppressor cells of normal mice and in a murine model of chronic hepatitis B virus. Clin. Exp. Immunol. 2011, 166, 134–42, doi:10.1111/j.1365-2249.2011.04445.x.
15. Yu, J.; Du, W.; Yan, F.; Wang, Y.; Li, H.; Cao, S.; Yu, W.; Shen, C.; Liu, J.; Ren, X. Myeloid-derived suppressor cells suppress antitumor immune responses through IDO expression and correlate with lymph node metastasis in patients with breast cancer. J. Immunol. 2013, 190, 3783–97, doi:10.4049/jimmunol.1201449.
16. Masuda, J.; Takayama, E.; Strober, W.; Satoh, A.; Morimoto, Y.; Honjo, Y.; Ichinohe, T.; Tokuno, S. I.; Ishizuka, T.; Nakata, T.; Mizutani, A.; Umemura, N.; Kitani, A.; Fuss, I. J.; Shigehiro, T.; Kawaki, H.; Mizuno-Kamiya, M.; Kondoh, N.; Seno, M. Tumor growth limited to subcutaneous site vs tumor growth in pulmonary site exhibit differential effects on systemic immunities. Oncol. Rep. 2017, 38, 449–455, doi:10.3892/or.2017.5646.
17. D'Antò, V.; Eckhardt, A.; Hiller, K.-A.; Spagnuolo, G.; Valletta, R.; Ambrosio, L.; Schmalz, G.; Schweikl, H. The influence of Ni(II) on surface antigen expression in murine macrophages. Biomaterials 2009, 30, 1492–1501, doi:10.1016/j.biomaterials.2008.12.004.
18. Bronte, V.; Pittet, M. J. The spleen in local and systemic regulation of immunity. Immunity 2013, 39, 806–18, doi:10.1016/j.immuni.2013.10.010.
19. Gabrilovich, D. I.; Nagaraj, S. Myeloid-derived suppressor cells as regulators of the immune system. Nat. Rev. Immunol. 2009, 9, 162–74, doi:10.1038/nri2506.
20. Masuda, J.; Takayama, E.; Strober, W.; Satoh, A.; Morimoto, Y.; Honjo, Y.; Ichinohe, T.; Tokuno, S.-I.; Ishizuka, T.; Nakata, T.; Mizutani, A.; Umemura, N.; Kitani, A.; Fuss, I. J.; Shigehiro, T.; Kawaki, H.; Mizuno-Kamiya, M.; Kondoh, N.; Seno, M. Tumor growth limited to subcutaneous site vs tumor growth in pulmonary site exhibit differential effects on systemic immunities. Oncol. Rep. 2017, 38, 449–455, doi:10.3892/or.2017.5646.
21. Chanmee, T.; Ontong, P.; Konno, K.; Itano, N. Tumor-Associated Macrophages as Major Players in the Tumor Microenvironment. Cancers (Basel). 2014, 6, 1670–1690, doi:10.3390/cancers6031670.
22. Thäle, C.; Kiderlen, A. F. Sources of interferon-gamma (IFN-gamma) in early immune response to Listeria monocytogenes. Immunobiology 2005, 210, 673–83.
23. Kanevskiy, L. M.; Telford, W. G.; Sapozhnikov, A. M.; Kovalenko, E. I. Lipopolysaccharide induces IFN-γ production in human NK cells. Front. Immunol. 2013, 4, 11, doi:10.3389/fimmu.2013.00011.
24. Wang, N.; Liang, H.; Zen, K. Molecular mechanisms that influence the macrophage m1-m2 polarization balance. Front. Immunol. 2014, 5, 614, doi:10.3389/fimmu.2014.00614.
25. Ostrand-Rosenberg, S.; Sinha, P.; Beury, D. W.; Clements, V. K. Cross-talk between myeloid-derived suppressor cells (MDSC), macrophages, and dendritic cells enhances tumor-induced immune suppression. Semin. Cancer Biol. 2012, 22, 275–81, doi:10.1016/j.semcancer.2012.01.011.
26. Lenczowski, M. J.; Van Dam, A. M.; Poole, S.; Larrick, J. W.; Tilders, F. J. Role of circulating endotoxin and interleukin-6 in the ACTH and corticosterone response to intraperitoneal LPS. Am. J. Physiol. 1997, 273, R1870-7.

27. Turner, P. V; Brabb, T.; Pekow, C.; Vasbinder, M. A. Administration of substances to laboratory animals: routes of administration and factors to consider. J. Am. Assoc. Lab. Anim. Sci. 2011, 50, 600–13.
28. Weiskopf, K.; Ring, A. M.; Ho, C. C. M.; Volkmer, J.-P.; Levin, A. M.; Volkmer, A. K.; Ozkan, E.; Fernhoff, N. B.; van de Rijn, M.; Weissman, I. L.; Garcia, K. C. Engineered SIRPα variants as immunotherapeutic adjuvants to anticancer antibodies. Science 2013, 341, 88–91, doi:10.1126/science.1238856.
29. Feng, M.; Chen, J. Y.; Weissman-Tsukamoto, R.; Volkmer, J.-P.; Ho, P. Y.; McKenna, K. M.; Cheshier, S.; Zhang, M.; Guo, N.; Gip, P.; Mitra, S. S.; Weissman, I. L. Macrophages eat cancer cells using their own calreticulin as a guide: roles of TLR and Btk. Proc. Natl. Acad. Sci. U. S. A. 2015, 112, 2145–50, doi:10.1073/pnas.1424907112.
30. Martinez, F. O.; Gordon, S. The M1 and M2 paradigm of macrophage activation: time for reassessment. F1000Prime Rep. 2014, 6, 13, doi:10.12703/P6-13.
31. Lanier, L. L. Natural Killer Cells: From No Receptors to Too Many. Immunity 1997, 6, 371–378, doi:10.1016/S1074-7613(00)80280-0.
32. Park, Y.-J.; Song, B.; Kim, Y.-S.; Kim, E.-K.; Lee, J.-M.; Lee, G.-E.; Kim, J.-O.; Kim, Y.-J.; Chang, W.-S.; Kang, C.-Y. Tumor microenvironmental conversion of natural killer cells into myeloid-derived suppressor cells. Cancer Res. 2013, 73, 5669–81, doi:10.1158/0008-5472.CAN-13-0545.
33. Weide, B.; Martens, A.; Zelba, H.; Stutz, C.; Derhovanessian, E.; Di Giacomo, A. M.; Maio, M.; Sucker, A.; Schilling, B.; Schadendorf, D.; Büttner, P.; Garbe, C.; Pawelec, G. Myeloid-derived suppressor cells predict survival of patients with advanced melanoma: comparison with regulatory T cells and NY-ESO-1- or melan-A-specific T cells. Clin. Cancer Res. 2014, 20, 1601–9, doi:10.1158/1078-0432.CCR-13-2508.
34. Kang, K.; Park, S. H.; Chen, J.; Qiao, Y.; Giannopoulou, E.; Berg, K.; Hanidu, A.; Li, J.; Nabozny, G.; Kang, K.; Park-Min, K.-H.; Ivashkiv, L. B. Interferon-γ Represses M2 Gene Expression in Human Macrophages by Disassembling Enhancers Bound by the Transcription Factor MAF. Immunity 2017, 47, 235–250.e4, doi:10.1016/J.IMMUNI.2017.07.017.
35. Zheng, X.-F.; Hong, Y.-X.; Feng, G.-J.; Zhang, G.-F.; Rogers, H.; Lewis, M. A. O.; Williams, D. W.; Xia, Z.-F.; Song, B.; Wei, X.-Q. Lipopolysaccharide-Induced M2 to M1 Macrophage Transformation for IL-12p70 Production Is Blocked by Candida albicans Mediated Up-Regulation of EBI3 Expression. PLoS One 2013, 8, e63967, doi:10.1371/journal.pone.0063967.
36. Nagaya, R.; Mizuno-Kamiya, M.; Takayama, E.; Kawaki, H.; Onoe, I.; Tanabe, T.; Nagahara, K.; Kondoh, N. Mechanisms of the immunosuppressive effects of mouse adipose tissue-derived mesenchymal stromal cells on mouse alloreactively stimulated spleen cells. Exp. Ther. Med. 2014, 7, 17–22, doi:10.3892/etm.2013.1382.